J. Int. Financ. Markets Inst. Money 88 (2023) 101837

Contents lists available at ScienceDirect

Journal of International Financial Markets, Institutions & Money

journal homepage: www.elsevier.com/locate/intfin

Review

The impact of crisis periods and monetary decisions of the Fed and the ECB on the sovereign yield curve network

Milan Csaba Badics[1], Zzsuzsa R. Huszar[1], Balazs B. Kotro *,[1]

Corvinus University of Budapest, Department of Investments, Fovam Square, Budapest, 1093, Hungary

ARTICLE INFO

JEL classification:
C32
G01
G12
G15
E52

Keywords:
Connectedness
Sovereign yield curve network
Toda–Yamamoto causality
Global and local crises
Fed monetary decisions

ABSTRACT

This study investigates the sovereign yield curve network of 12 developed countries. We decompose the term structure of interest rates into the Level, Slope, and Curvature factors using the Diebold and Li (2006) model. The connections between the latent yield curve factors across the countries are measured using the Toda and Yamamoto (1995) model, which is suitable for cointegrated time series. Our timeframe covers more than 23 years; therefore, we are able to compare two global and two local crisis periods. For deeper understanding the structural changes, and identify the key participants in the sovereign yield curve network, we analyze the connections on factor, country, and node levels. Investigating the network on node level, in the entire sample period, all three US latent factors act as key participants in our network, however, their contribution is time variant. We find that local and global crises behave differently. The network density differences on average are relatively small across calm and local crises periods, but significantly larger during the Global Financial Crisis and the European sovereign debt crises. Furthermore, we explore links between the easing and tightening decisions by the Fed and the ECB, and the time-varying dominance of the US yield curve in our sovereign yield curve network. The dominance of the US factors peaks if the Fed leads the hiking cycle and reaches its minimum when the interest rate cycle is led by the ECB.

1. Introduction

Over the past few decades interlinkages between global financial markets increased due to the fundamentals, regulatory convergence, and growing international trade. Globalization and surging connectedness led to a higher likelihood of local and global crises. Furthermore, during turbulent periods the strength of connections sharply increases, and risk spills over across markets and asset classes, as it happened during the Dotcom Bubble, the Global Financial Crisis of 2007–2009, the European Sovereign Debt Crisis, or the recent Covid-19 Pandemic. Examining financial systems is crucial for investors and other market participants too because a shock and a crisis in one market can affect the return and volatility of another market and infect the decision-making for portfolio risk management. For this reason, it is essential for regulators to monitor the rapid changes, understand the network dynamics on different levels, and identify the key participants of financial networks. During the last few years, motivated by these episodes of crises, the connections between financial markets have been widely investigated in academia, especially from a network perspective (Diebold and Yilmaz, 2009; Billio et al., 2012).

* Corresponding author.
E-mail addresses: milancsaba.badics@uni-corvinus.hu (M.C. Badics), zsuzsareka.huszar@uni-corvinus.hu (Z.R. Huszar), balazsbence.kotro@uni-corvinus.hu (B.B. Kotro).

[1] Badics, Huszar and Kotro are from the Finance Institute at Corvinus University of Budapest. Huszar is also affiliated with Department of Finance at NUS Business School, at the National University of Singapore.

https://doi.org/10.1016/j.intfin.2023.101837
Received 1 February 2023; Accepted 29 August 2023
Available online 9 September 2023

To examine financial networks, several approaches have appeared in the literature since the Global Financial Crisis. On the theoretical side, Gai and Kapadia (2010), Gai et al. (2011), Elliott et al. (2014), Acemoglu et al. (2015) and Glasserman and Young (2015) analyze the effects of financial contagion on risk. On the empirical side, there are various ways to quantify connectedness. In the last decade, the widespread methods are the Granger causality (Billio et al., 2012), Conditional Value at Risk (CoVaR) (Adrian and Brunnermeier, 2011), Systemic Expected Shortfall (SES) and Marginal Expected Shortfall (MES) (Acharya et al., 2012), and the spillover measure based on Forecast error variance decompositions (FEVD) from Vector autoregressive (VAR) model, shown by Diebold and Yilmaz (2009, 2012) and Diebold and Yılmaz (2014). These techniques are frequently used to examine networks in various asset classes, such as equities (Bernal et al., 2014; Vỳrost et al., 2015; Billio et al., 2016; BenSaïda, 2019), bonds (Antonakakis and Vergos, 2013; Reboredo and Ugolini, 2015; Corsi et al., 2018), currency rates (Bubák et al., 2011; Antonakakis, 2012; Ji et al., 2019) or commodity prices (Kang et al., 2017; Ji et al., 2018; Umar et al., 2021b). The Granger and FEVD-based frameworks have the benefit over CoVaR and MES approaches in that they can better analyze the network on different levels (pairwise, subsystem and total connectedness, Diebold and Yılmaz (2014)). The Granger causality and the Diebold–Yilmaz (D–Y) approaches are extensively used in the network literature (Barigozzi and Brownlees, 2019).

The network-related econometrics frameworks are increasingly evolving (Baruník and Křehlík, 2018; Demirer et al., 2018). Despite the high number of recent connectedness-related articles and the widespread methods, the deeper structure of the networks (analyzing on different levels) has been investigated by far fewer. In addition to that, only a few studies (Hautsch et al., 2015; Sedunov, 2016; Nucera et al., 2016; Hué et al., 2019) try to identify the key participants of the financial networks and. Although there is a large body of both theoretical (Gai and Kapadia, 2010; Gai et al., 2011) and empirical (Diebold and Yilmaz, 2012; Alter and Beyer, 2014; Bouri et al., 2021) literature focusing on differences between calm and turbulent periods, the comparison of different crises has only come into focus in recent years (e.g. Mensi et al. (2018), Gunay (2021), Batten et al. (2022), Jebabli et al. (2022), Jana et al. (2022) and Baumöhl et al. (2022)).

The majority of the network-related literature focuses on equities and fewer papers turn attention toward sovereign bonds. Given that two recent crises, which had serious, cross-county impacts, have been closely related to the fixed-income market (namely, the Subprime and the European Sovereign Debt Crises), a study that focuses on sovereign yield curves is essential. While researchers focus mainly on the links between sovereign yields of European (Antonakakis and Vergos, 2013; Fernández-Rodríguez et al., 2015) or Asian (Gabauer et al., 2022) countries, only a few studies explore the connections between the most developed (Umar et al., 2022; Berardi and Plazzi, 2022) markets. Additionally, the most developed sovereign bond markets have significant influences on the yield curves of other countries, as shown by Ahmad et al. (2018) and Stona and Caldeira (2019).

In this paper, to address the gap in the empirical literature, we calculate the yield curve factors (Level, Slope, and Curvature) of 12 developed sovereigns based on the model of Diebold and Li (2006) and investigate the connectedness among them from 1998 to 2021. Our examination covers cross-factor relations as well, and we use the Toda and Yamamoto (1995) causality test to handle cointegrated time series. We are particularly interested in investigating the density of networks during calm and turbulent periods. To deeper understand the structural changes and identify the key participants in the sovereign yield curve network, we analyze the connections on factor, country, and node level. In addition, in analyzing the nodes' connections, we examine the relation between the monetary policy decisions and the sovereign yield curve network. We explore links between the easing and tightening decisions by the Fed and ECB, and the time-varying dominance of the key participants in the sovereign yield curve network.

The contribution of this paper to the existing literature is fourfold. First, to our knowledge, we are the first to adopt the Toda and Yamamoto (1995) causality test to examine a large network of sovereign yield curves over an extended period of time. While the Time-Varying Parameter Vector Autoregression (TVP-VAR) model recently suggested choice for network analysis (Rossi, 2005; Rossi and Wang, 2019), our choice of the Toda–Yamamoto model (T-Y hereafter) is motivated by its simplicity and flexibility (see Rambaldi and Doran (1996)), alleviating complications that may arise from using TVP-VAR with cointegrated series. The T-Y causality test is applicable regardless of whether a series is $I(0)$, $I(1)$, or $I(2)$ are cointegrated or not cointegrated in any arbitrary order. The procedure avoids the bias associated with unit roots and cointegration tests (Rambaldi and Doran, 1996; Zapata and Rambaldi, 1997; Clarke and Mirza, 2006), as it does not require pre-testing of the cointegrating properties of the system. Consistent with earlier studies (e.g., Cavaliere et al. (2010); Engsted and Tanggaard (1994), Hall et al. (1992) and Wilms and Croux (2016)), we also provide evidence of numerous cointegrated time-series yield curve pairs using Engle and Granger (1987) and Johansen (1988) tests. To address potential limitations of T-Y model, and account for potentially time-varying parameters in the network, we use 750-day estimation moving window estimation during the sample period.

Second, using a large sample of sovereign yield curves, from 12 countries over 23 years, we consider Level, Slope, and Curvature factors using the Diebold and Li (2006) model.[2] We explore cross-connections between sovereign yield curve factors and show evidence of a significant amount of linkage between the Level Slope and Curvature subnetworks. We identify the key participants in the sovereign yield curve network and find that the US factors dominate as key network participants throughout the sample, in each subperiod, with some variation across time. These results extend the findings of other recent yield curve papers (e.g., Cavaca and Meurer (2021); Umar et al. (2021a, 2022) and Gabauer et al. (2022)) who examine spillover effects among networks created from Level, Slope and Curvature factors only and do not identify the top nodes in the system.

[2] Our model is a close network approach, containing only yield curve factor data, as we focus on the endogenous relationships. Therefore omitted variable bias might occur.

Third, we provide several unique insights by analyzing the deeper structure of our network showing the followings: (1) the two global crises have more dense networks, than the local ones;[3] (2) US latent factors act as key participants in our network, however, their contribution is time variant; (3) cointegrated relationship between Canada and US results in the Canada being co-driver in the network during in crises periods.

Lastly, we contribute to the literature about the spillover effect of monetary policy decisions (e.g., Hofmann and Takáts (2015); Kearns et al. (2018), Albagli et al. (2019), Lakdawala et al. (2021), Miranda-Agrippino and Ricco (2021), Jarociński (2022) and Miranda-Agrippino and Nenova (2022)) and provide insights for monetary policy discussions. We also extend the scope of the earlier sovereign yield curve studies as we inspect the dynamics of the key participants' dominance in the network and connect these dynamics to the monetary policy decisions. Specifically, by analyzing the influence of the easing and tightening decisions by the Fed and the ECB on the key participants of the sovereign yield curve network we find that the dominance of the US factors peaks if the Fed leads the rate hike cycle and reaches its minimum when the interest rate cycle is led by the ECB. We provide insights for the more exposed market participants to prepare for the expected impacts of US intervention potentially better. We also highlight the potential structural breaks in crisis and tranquil periods, by showing that Canada is effectively an extension of US monetary policy impact during crisis periods, highlighting the importance of close trade partner relations.

The rest of this paper is structured as follows. In Section 2 we review the literature on the sovereign yield curve networks, in Section 3 we discuss the methodology for extracting the latent factors with the Diebold–Li model and we introduce the T-Y model. In Section 4 the data is presented, in Section 5 we discuss our empirical results and in Section 6, we conclude and present the policy implications.

2. Literature review

There are two families of articles investigating links among sovereign bonds. The first one examines the market integration and comovements between short and long-term yields of international bonds. The second one estimates the connectedness among sovereign yields or yield curve factors with network-based econometric methods.

An overview of existing literature on the bond market reveals that there are only two pioneer studies that analyze the connectedness of international bond markets from a network view, without using the last 10 years' network-based econometrics methodologies. In an early paper, Sander and Kleimeier (2003) investigate connections among Asian sovereign bond spreads with Granger-causality during four episodes of Asian crisis. They show that the Asian crisis changed causality patterns on a regional base. Christiansen (2007) examine the volatility spillover between the US and European sovereign bond markets using a GARCH model. Results indicate volatility spillover from the US to European bond markets, but not vice versa.

Since the GFC network-based methodologies have gained popularity. Antonakakis and Vergos (2013) examine the spillover in the sovereign yield spread among Eurozone countries using measures developed by Diebold and Yilmaz (2012) and find that more than 60% of the variances are explained by spillovers from other countries. Gómez-Puig and Sosvilla-Rivero (2013) analyze the time-varying nature of Granger causal relationships between the yields on 10-year government bonds issued by five EMU countries. In a similar study (Gómez-Puig and Sosvilla-Rivero, 2016), using sovereign bond yield spreads of ten central and peripheral countries to examine the dynamic evolution of Granger causality network connections. Both studies document peaks of linkages during the ESDC. Claeys and Vašíček (2014) measure the direction of the linkages of the sovereign bond market among sixteen European Union countries, using a factor-augmented version of the D–Y model. They show that spillover effects from other countries dominate the domestic fundamental factors for EMU countries' sovereign yields. Fernández-Rodríguez et al. (2015) investigate 10-year yield volatility spillovers in eleven Eurozone countries using the D–Y framework. They document that more than half of the total variance of the forecast errors is explained by systemic shocks. A year later in Fernández-Rodríguez et al. (2016) study the time-varying integration of EMU bonds with the same framework. Contrary to previous empirical studies, they find a significant decrease in connectedness during the crisis period. Reboredo and Ugolini (2015) use conditional value-at-risk (CoVaR) to measure systemic risk in European sovereign bond markets around the ESDC. They find that prior to the crisis, the markets were all coupled, while after that, the risk decreased for the affected countries. Bernal et al. (2016) use the same methodology to analyze the risk spillovers within the EMU and examine the impact of Economic Policy Uncertainty to the net connections. They find that uncertainty has an impact to country-level spillovers which is stronger for key countries. Using Diebold–Yilmaz-based structural vector autoregressions, De Santis and Zimic (2018) examine the bond market connectivity among the 10-year sovereign yields of 12 developed countries. They document that connectedness among sovereign bond yields declined during the 2008–2012 period due to financial fragmentation. Chatziantoniou and Gabauer (2021) concludes the same while examining the financial risk synchronization of 11 EMU members' government bond yields with a time-varying parameter Diebold–Yilmaz model. They document fragmentation during the ESDC and find that core countries spillover risk shocks to periphery countries. Hamill et al. (2021) investigate the network connectivity of the European sovereign bond markets and compare the different variants of D–Y frameworks. They document that the Lanne–Nyberg dynamic connectedness model provides an accurate indication of the GFC. In a recent study, Benlagha and Hemrit (2022) investigate the impact of Economic Policy Uncertainty (EPU) on the connectedness among G7 sovereign bond yields. They find that EPU affects the connectedness of long-term yields but is insignificant for short-term yield spillovers. Berardi and Plazzi

[3] We examine the Dotcom Bubble (DCB), the Global Financial Crisis (GFC), the European Sovereign Debt Crisis (ESDC), and the Covid-19 Pandemic (C19). From these, we consider the GFC and the C19 Pandemic as global, while the other two as local crises. It is revealed that the two global crises have more connection counts, than the local ones.

(2022) investigate the connectedness between the yield curve components of four developed countries after they decompose the nominal yields into the sum of expectations, the term premium, and the convexity term. They find that the USA indicates the strongest spillovers in long-term yields.

While the above mentioned studies investigate the linkages among government bond yields in the last few years, another strand of literature analyze yield curve factor connectedness among sovereign markets.

Sowmya et al. (2016) are the first to investigate linkages across latent factors of yield curves using D–Y framework in a sample of four developed and seven emerging Asian economies. They find that the regional influence is higher in Slope and Curvature factors among the Asian countries. In a recent paper, Umar et al. (2021a) study connectedness of 11 Eurozone countries and document that the core countries are net transmitters while the peripheral countries are net receivers. Cavaca and Meurer (2021) examine the spillover between yield curve factors of the United States and four South American countries. They prove that the degree of spillover is highest for the Slope subnetwork, followed by the Level and the Curvature. Gabauer et al. (2022) explore the spillover of yield curve factors across the Asia-Pacific sovereign bond markets with a time-varying parameter D–Y model. They find that the highest market connectedness is in the Level subsystem followed by the Slope and Curvature subnetworks. Umar et al. (2022) examine the connectedness between the Level, Slope, and Curvature factors individually. They conclude that France and Germany are the transmitters whereas the UK and Japan are the net receivers for all the yield curve components' networks.

We briefly summarize and highlight the gaps in the literature in A.1. As of today, a large number of connectedness studies use VAR-based Diebold–Yilmaz frameworks despite the concern that the application of the VAR model on cointegrated time series can lead to spurious connections. A notable exception is Cavaca and Meurer (2021)'s work where the authors try to handle this problem within the estimation of the network model. However, unlike the Vector Error Correction Model (VECM)-based (D–Y) approach, which relies on the variables being integrated in the same order for cointegration analysis, the T-Y model does not require such an assumption. Although there is a large number of recent sovereign bond connectedness-related studies, deep structural network analysis, examination networks at multi-levels (analyzing on different levels), is scarce. The papers analyze the network either on node- or on factor level. Lastly, while a number of bond market works compare tranquil and turbulent periods without specific distinction in crisis periods, comparing different crisis periods and exploring the network behavior of key market players are underrepresented in the literature.

3. Methodology

Our approach consists of two steps. First, the Diebold and Li (2006) methodology is used to decompose the yield curve into latent and economically meaningful factors. Next, we quantify the significant causality relations between the different yield curve components using the Toda and Yamamoto (1995) model. We describe both of these processes in the next subsections.

3.1. The Nelson–Siegel yield curve model and the Diebold–Li decomposition

Nelson and Siegel (1987) (N-S hereafter) suggest a flexible, parsimonious, exponential components framework that has the ability to capture a variety of frequently observed yield curve shapes (forward sloping, inverse, humped) and allows for a clear interpretation of the estimated factors. Diebold and Li (2006) (D-L hereafter) extend the N-S approach, by allowing the dynamic change of the latent factors. A central feature of the model is that these factors can be interpreted as the Level, Slope, and Curvature as proven by Diebold et al. (2006), Mumtaz and Surico (2009), Mönch (2012), Koopman et al. (2010) and Christensen and Rudebusch (2012). Following N-S and D-L, we assume that these components include the majority of the information in the term structure of the yield curve. The D-L model offers an adaptable structure and has a wide applicability in any market (Yu and Zivot, 2011; Xu et al., 2019; Bredin et al., 2021).

The observed yield curve can be described with the following equation:

$$y_\tau = \beta_1 + \beta_2 \left(\frac{1 - e^{-\lambda\tau}}{\lambda\tau} \right) + \beta_3 \left(\frac{1 - e^{-\lambda\tau}}{\lambda\tau} - e^{-\lambda\tau} \right) \tag{1}$$

where y_τ denote yields for τ maturity, β_1, β_2 and β_3 are the Level, Slope, and Curvature parameters respectively, and λ is a parameter that controls the shapes of loadings for the D-L factors (especially for Curvature). The β_i parameters have an economic meaning: β_1 (Level) represents the long end of the yield curve, β_2 (Slope) is the short-term component, while β_3 (Curvature) mimics the middle interval. The Level factor applies equally to all maturities. Some of the articles focus on the Level and Slope factors only, however, De Pooter (2007), Almeida et al. (2009) and Ullah et al. (2015) draw attention to the importance of the third factor, therefore we involve Curvature in our analysis.

We estimate the latent factors using the two-step procedure on a daily basis proposed and applied by Diebold and Li (2006). We use simple ordinary least squares (OLS) on every day to extract the time-varying latent Level, Slope, and Curvature factors. Following Diebold and Li (2006), Bianchi et al. (2009), Koopman et al. (2010) and Van Dijk et al. (2014) we set the λ parameter at 0.06093 such that the Curvature factor attains its maximum at $\tau = 30$ months.

3.2. The Toda–Yamamoto model

The T-Y model is a popular causality testing approach, introduced by Toda and Yamamoto (1995). Over the past few years several network-based studies applied the T-Y model to handle cointegrated time series (Gündüz and Kaya, 2014; Bratis et al., 2020; Nazlioglu et al., 2020). As T-Y point out, the classic Granger causality test (Granger, 1969) obtained by a VAR model on cointegrated time series can lead to spurious connections (Dolado and Lütkepohl, 1996; Zapata and Rambaldi, 1997; Pittis, 1999). The T-Y approach eliminates this shortcoming by introducing a modified Wald test (MWald) which has restrictions on the parameters of the VAR(p) model. The test is based on a χ_p distribution, where $p' = p + d^{max}$. The order of VAR is increased artificially, p gets increased by d^{max} which is the maximal order of the integration. Then, a VAR with an order of $(p + d^{max})$ is estimated, where the last d^{max} lag coefficient is ignored. A VAR($p + d^{max}$) model is described by Eqs. (2) and (3):

$$Y_t = \alpha_0 + \sum_{i=1}^{p} \delta_{1i} Y_{t-i} + \sum_{j=p+1}^{d^{max}} \alpha_{1j} Y_{t-j} + \sum_{j=1}^{p} \theta_{1j} X_{t-j} + \sum_{j=p+1}^{d^{max}} \beta_{1j} X_{t-j} + \omega_{1t} \tag{2}$$

$$X_t = \alpha_1 + \sum_{i=1}^{p} \delta_{2i} Y_{t-i} + \sum_{j=p+1}^{d^{max}} \alpha_{2j} Y_{t-j} + \sum_{j=1}^{p} \theta_{2j} X_{t-j} + \sum_{j=p+1}^{d^{max}} \beta_{2j} X_{t-j} + \omega_{2t} \tag{3}$$

where α, δ, θ, and β are model parameters, p is the optimal lag of the original VAR model, ω_{1t} and ω_{2t} are the errors of the VAR model, and d^{max} is the maximal integration order in terms of the T-Y model. Hereby based on (2), there is a Granger causality between X and Y, $\delta_{1i} \neq 0$ for all i. In the same way, based on (3), Granger causality is observable between Y and X, if $\delta_{2i} \neq 0$ for all i.

From the VAR($p + d^{max}$) model, the T-Y model is realized in three steps:

- Perform d^{max} ordered stationarity tests on all of the time series by applying ADF (Augmented Dickey–Fuller test), KPSS (Kwiatkowski–Phillips–Schmidt–Shin test), and PPE (Phillips–Perron test) tests individually or in combination.
- Determine the optimal lag, (p) with the maximal consistency of the AIC (Akaike's Information criterion), BIC (Bayesian Information Criterion), the HQ (Hannan–Quinn criterion), or the LR (Likelihood Ratio test) criteria.
- With the application of the upper-mentioned parameters, rejecting the Granger test between X and Y means a causality relation in Toda–Yamamoto terms. Bivariate rejection suggests a mutually causal relation between the variables.

4. Data

Following Sowmya et al. (2016), Hamill et al. (2021), Umar et al. (2022) and Stenfors et al. (2022), we collect daily data from twelve developed countries. We select sovereigns with the highest GDPs and liquid bond markets, resulting in the sample dataset: Australia, Canada, Switzerland, Germany, Spain, France, Great Britain, Italy, Japan, South Korea, the Netherlands, and the United States of America.[4] Similarly to Antonakakis and Vergos (2013), Sowmya et al. (2016), Byrne et al. (2019), Umar et al. (2022) and Gabauer et al. (2022), we collect the zero-coupon sovereign bond yields from Bloomberg. The specific yield curves and the corresponding tickers are listed in Table A.2 in Appendix. We consider 15 maturities[5] to obtain the yield curve factors of the term structure for each country as Umar et al. (2021a, 2022) and we extend the analysis of Sowmya et al. (2016), Cavaca and Meurer (2021) and Gabauer et al. (2022) who use shorter terms only. The time period is from September 30, 1998, to December 31, 2021. Our sample spans over various business cycle phases and major turbulent periods too. Based on Byrne et al. (2019) and Bouri et al. (2021) we cover the following crisis periods:[6]

- The Dotcom Bubble (DCB): 03/10/2000–12/02/2001
- The Global Financial Crisis (GFC): 09/15/2008–07/21/2010
- The European Sovereign Debt Crisis (ESDC): 11/21/2010–03/13/2013
- The Covid-19 Pandemic (C19): 01/20/2020–12/31/2021

and two longer calm periods (CALM1, CALM2) between these crises.[7] According to our best knowledge, we are the first to examine the characteristics of four different crises on the bond market. We differentiate between global (GFC, C19) and local (DCB, ESDC) crises, as GFC and C19 are worldwide events as opposed to the other crises (DCB and ESDC) which primarily affect one country or a region.

The zero-coupon sovereign bonds are denominated in local currency and we use these yields for two reasons. As per (Cavaca and Meurer, 2021), debt in local currency better represents the different interest rate cycles of the economy and the domestic monetary policy. Additionally, according to Sowmya et al. (2016), local currency denominated bonds have better liquidity than debt issued in US dollars.

Descriptive statistics for the 1-, 5-, 10- and 30-year nodes of each country's yield curve are provided in Table A.4 of the Appendix. The yield curve characteristics are in line with the findings of previous studies (Sowmya et al., 2016; Cavaca and Meurer, 2021).

[4] The countries are frequently referred to by the three-letter shorthand created by the OECD so henceforth we use AUS, CAN, CHN, DEU, ESP, FRA, GBR, ITA, JPN, KOR, NLD, and USA.

[5] 3, 6, 12, 24, 36, 48, 60, 72, 84, 96, 120, 180, 240, and 360 months.

[6] Start dates and end dates of such crises are linked to global events, described in A.3 in the Appendix. Our results are robust to the choice of the selected dates. The results of this robustness analysis are not reported here but are available from the authors upon request.

[7] CALM1: 12/03/2001–09/14/2008; CALM2: 03/14/2013 - 01/19/2020. Before the Dotcom Bubble, there is an additional calm period (CALM0), due to the rolling window estimation in the dynamic analysis we do not provide results from this era. The timeframe between GFC and ESDC is very short, therefore we do not consider it as a separate subperiod.

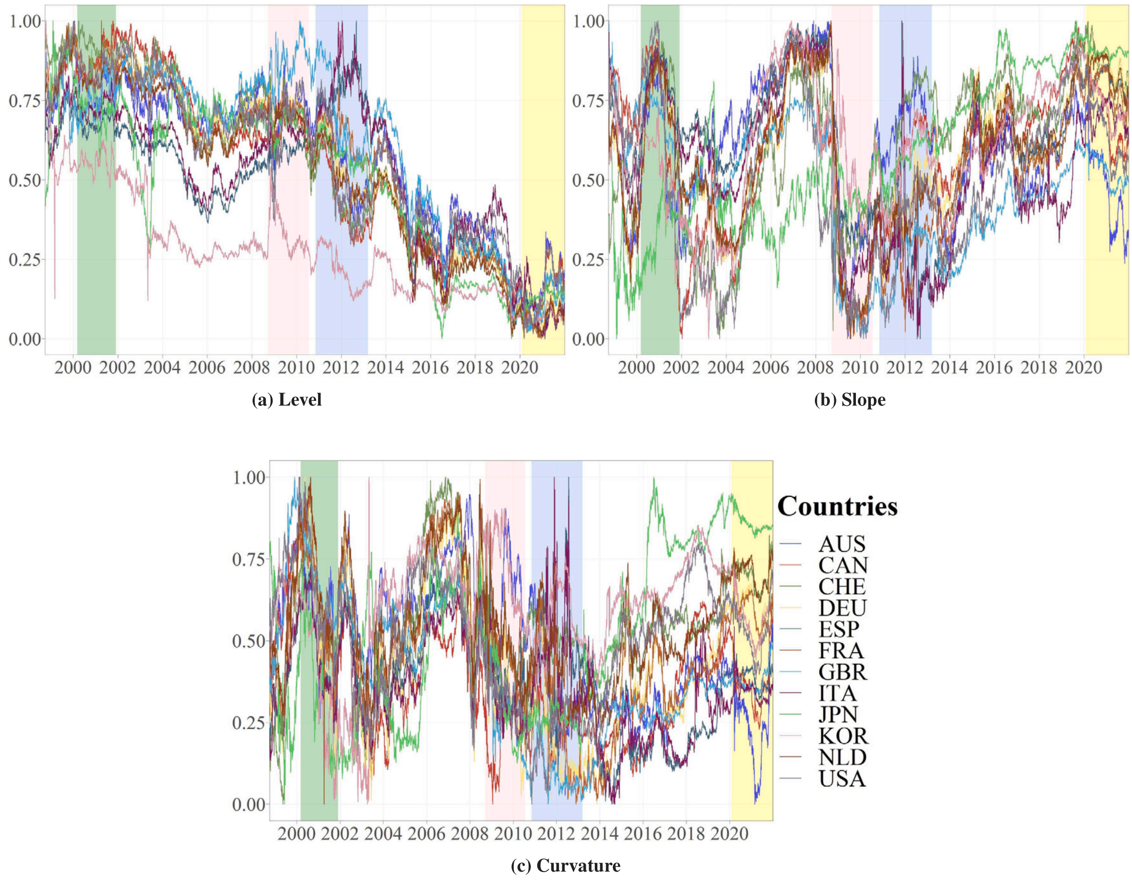

Fig. 1. Normalized time series of Level, Slope, and Curvature factors. Notes: The green area denotes the DCB, the red-shaded area shows the GFC, the blue field represents the ESDC and the yellow area the C19 period. (For interpretation of the references to color in this figure legend, the reader is referred to the web version of this article.)

The normalized time series of the D-L factors are shown in Fig. 1 in which, DCB is depicted in green shading, GFC is denoted with red, ESDC is represented with blue, and C19 is marked with yellow.

Fig. 1 sheds light on several stylized facts. Level factors decline and converge across countries during the examination period. Evans and Marshall (2007) find evidence from the USA market that macro shocks shift the level factor of the yield curve, which is visible in our sample too, during the GFC and ESDC in 1(a). Slope time series show countercyclical behavior and comoves across countries. As per (Diebold et al., 2006), the curvature factor has only weak links with the macroeconomic fundamentals thus trends or cyclicality are less specific for this factor.

The descriptive statistics of the estimated D-L factors are represented in Table 1. The average Level factors are positive in all cases, with South Korea having the highest values and Japan the lowest. The mean Slope is negative for all countries, which refers to the typical upward-sloping shape of the yield curves. In absolute terms, Italy has the highest Slope, while Australia has the lowest. The average Curvature is also negative, highest for Italy and lowest for Great Britain (in absolute terms).

We employ the Jarque–Berra test statistics for the normality test, which is always rejected. Furthermore, the ADF and KPSS unit-root tests for stationarity are applied. The Level time series is stationary for Korea and the USA, the Slope for Japan, and Curvature for Australia and Italy on a 99% confidence level, according to the ADF test. According to the KPSS test, neither of the time series is stationary. The first difference is stationary for all time series based on the two tests. The results of the ADF and KPSS tests are in the Appendix in Table A.5.

Pairwise Engle and Granger (1987) and Johansen (1988) tests are used to determine cointegrations before using the first differences for further analysis. The ratios of the cointegrated time series, grouped by factors, are shown in Table 2.

Table 2a and b provide a high ratio of cointegrated connections, for example, the Level-Curvature subsystem is greater than 80% in both cases. Based on Table 2 and Table A.5 of the Appendix, applying the T-Y model is required because the time series are not stationary in the same order and the ratio of cointegrated time series is high.

Table 1
Descriptive statistics of the yield curve factors.

Factor	Average	Std. dev.	Minimum	Maximum	Jarque–Bera t-stat.	P value
Australia						
Level	4.87	1.50	1.06	7.71	540.29	0.00***
Slope	−1.11	0.99	−4.14	0.97	85.24	0.00***
Curvature	−2.15	1.90	−6.80	2.93	205.41	0.00***
Canada						
Level	3.94	1.56	0.70	6.62	404.33	0.00***
Slope	−1.83	1.37	−5.35	0.58	364.08	0.00***
Curvature	−2.18	1.94	−6.27	4.83	400.29	0.00***
Switzerland						
Level	2.19	1.56	−0.79	4.63	528.09	0.00***
Slope	−1.60	0.94	−4.10	−0.06	543.73	0.00***
Curvature	−2.71	1.49	−7.25	1.05	30.68	0.00***
Germany						
Level	3.35	1.98	−0.55	6.56	542.63	0.00***
Slope	−1.84	1.11	−4.69	0.22	234.39	0.00***
Curvature	−3.51	1.73	−6.81	0.96	256.80	0.00***
Spain						
Level	4.54	1.73	0.75	8.56	397.05	0.00***
Slope	−2.78	1.52	−7.35	−0.07	282.06	0.00***
Curvature	−4.01	2.09	−8.75	3.90	115.59	0.00***
France						
Level	3.72	1.80	0.11	6.63	575.05	0.00***
Slope	−2.15	1.17	−4.85	0.16	241.96	0.00***
Curvature	−3.98	1.90	−8.08	0.57	47.29	0.00***
Great Britain						
Level	3.69	1.37	0.47	5.77	764.03	0.00***
Slope	−1.39	1.73	−5.40	3.21	233.43	0.00***
Curvature	−1.82	3.58	−8.79	8.77	93.08	0.00***
Italy						
Level	4.83	1.43	1.43	7.90	481.67	0.00***
Slope	−3.01	1.39	−6.36	−0.24	196.68	0.00***
Curvature	−4.19	1.96	−8.74	4.06	142.96	0.00***
Japan						
Level	1.79	0.91	−0.03	3.57	599.64	0.00***
Slope	−1.43	0.75	−3.30	−0.09	318.65	0.00***
Curvature	−3.72	1.44	−6.54	−0.95	508.30	0.00***
South Korea						
Level	6.13	2.49	1.88	17.23	842.90	0.00***
Slope	−3.00	1.58	−7.85	0.10	169.56	0.00***
Curvature	−4.17	3.00	−14.38	2.67	1961.09	0.00***
The Netherlands						
Level	3.45	1.97	−0.36	7.01	539.12	0.00***
Slope	−1.95	1.14	−4.89	0.20	237.11	0.00***
Curvature	−3.30	1.57	−8.40	0.74	180.26	0.00***
USA						
Level	4.39	1.45	0.96	6.98	383.47	0.00***
Slope	−2.44	1.72	−5.71	0.91	311.13	0.00***
Curvature	−3.61	2.68	−10.35	3.27	197.93	0.00***

Notes: This table reports the descriptive statistics of latent factors for each country extracted from the Diebold–Li model. Jarque–Bera tests the normality of the distribution. Rejection of null hypothesis at 1%, 5%, and 10% levels are denoted by ***, **, and * respectively.

Table 2
Pairwise Engle–Granger and Johansen tests.

(a) Engle–Granger test				(b) Johansen test			
	Level	Slope	Curvature		Level	Slope	Curvature
Level	83.3%	41.7%	86.1%	Level	68.1%	88.9%	83.3%
Slope	16.0%	65.0%	90.3%	Slope	88.9%	88.9%	59.0%
Curvature	23.6%	61.1%	91.7%	Curvature	83.3%	59.0%	37.5%

Notes: Instead of the 36 × 36 matrix which we obtain from the pairwise Engle–Granger and Johansen tests, we show only the subsystems-based aggregated values in this table.

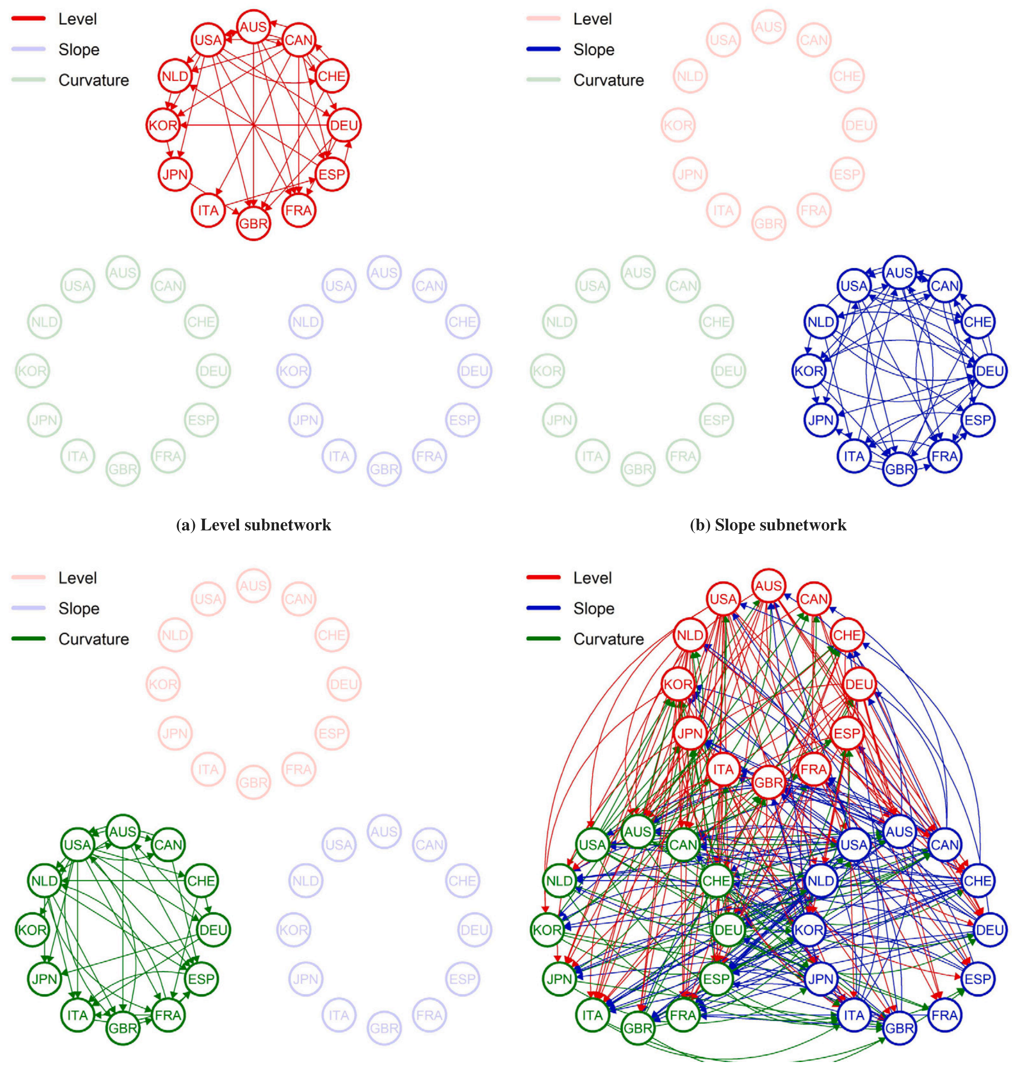

(a) Level subnetwork

(b) Slope subnetwork

(c) Curvature subnetwork

(d) Cross connections

Fig. 2. Causality relations within subnetworks, estimated by static Toda–Yamamoto model. Notes: Level factors are displayed in red, Slopes in blue, and Curvatures in green. An arrow between two factors indicates the direction of causation, and the color of the arrow indicates the source factor. Time series are differentiated at a maximum of one time, and the ideal lag time is chosen based on the AIC. For Level factors, 34; for Slope, 47; and for Curvature, 36 connections are significant from the possible $132 = (12 \times (12 - 1))$. In the case of cross-connections, 258 are significant from the possible $864 = (1260 - 3 \times 132)$. For total connections, 375 links are significant from the possible $1260 = (36 \times (36 - 1))$. (For interpretation of the references to color in this figure legend, the reader is referred to the web version of this article.)

5. Results

5.1. Static, full-sample connectedness analysis

Following Antonakakis and Vergos (2013), Claeys and Vašíček (2014), and Fernández-Rodríguez et al. (2015), we begin our analysis with a static investigation on a factor level. We measure the connections within the Level, Slope, and Curvature subsystems, and identify the cross-relations among them. Fig. 2 displays the causal linkages at a 1% level of significance, separated by subnetworks. The figure shows connections estimated by the Toda–Yamamoto procedure, using all the available data.

The Slope network has the highest density of the three subsystems with 35.61% of the potential relations being significant. It is followed by Curvature (27.27%), then Level (25.76%). The findings of Sowmya et al. (2016), Umar et al. (2021a, 2022) and Gabauer et al. (2022), who all claim that Level subsystem has the largest spillover effect, followed by Slope, and Curvature, are in contrast with ours. However, according to Cavaca and Meurer (2021), the Slope is the most connected subnetwork, which is supported by our findings. In addition to the different country set and the sample length, the other reason for the different results could be the T-Y

Table 3
The number and distribution of the significant connections defined in the system.

(a) Number of connections, grouped by factors					(b) Distribution of connections, grouped by factors				
	Level	Slope	Curvature	Outgoing		Level	Slope	Curvature	Outgoing
Level	34	43	48	125	Level	25.8%	29.9%	33.3%	29.8%
Slope	33	47	62	142	Slope	22.9%	35.6%	43.1%	33.8%
Curvature	34	38	36	108	Curvature	23.6%	26.4%	27.3%	25.7%
Incoming	101	128	146	375	Incoming	24.0%	30.5%	34.8%	29.8%

Notes: In the diagonal, we divide the connections by $132 = (12 \times (12-1))$, since this is the maximum definable relation in the subnetworks. Between two subsystems this number is $144 = (12 \times 12)$, we scale the upper and lower triangular by this. The values in the summarized row and column are divided by $420 = (132 + 144 + 144)$. The total definable connections in the network are $1260 = (420 \times 3)$, we divide 375 by this.

Table 4
Net and sum connections throughout the study period, aggregated by countries, ordered by net connections.

Country	Net connections	Sum connections
USA	**45**	89
DEU	**18**	74
AUS	16	80
CAN	11	69
CHE	9	51
NLD	2	58
KOR	−8	56
GBR	**−13**	59
ESP	−16	58
ITA	−18	60
JPN	**−22**	44
FRA	−24	50

model, which is suitable for filtering out spurious connections in the case of highly cointegrated systems (compared to the widely used VAR-based D–Y spillover index which is applied in the above-mentioned papers).

We also analyze the cross-connections among the yield curve components, for further insights. Altogether 258 significant cross-connections are defined, about 29.86% of the total 864 possible edges. From these connections, 95 (36.8%) originate from Slope-, 92 (35.3%) from Level-, and 72 (27.9%) from Curvature nodes. Altogether 258 significant cross-connections can be defined, which is 29.86% of the total possible edges of 864. From these, 95 (36.8%) originate from Slope, 92 (35.3%) from Level, and 72 (27.9%) from Curvature nodes. Based on Table 3a, on factor level, the Curvature has the most incoming edges, while the Slope has the most outgoing ones. The Level has the least incoming links while it is second in the list of outgoings. The Curvature subnetwork has the least outgoing edges, and in this sense, it is the least connected, which is in line with the findings of Dewachter and Lyrio (2006).

Fig. 2(d) and Table 3 highlight that the connections between different subsystems are not negligible. The cross-factor connections are 68.8% of the defined causality relations (258 out of 375).

Although Fig. 2 and Table 3 provide information about the subsystems of the factors, these are not sufficient to draw conclusions about the main economics drivers behind the network. To extend the factor level-based analysis in the next subsection we examine our sovereign yield curve network on a country and a node-wise level too.

5.1.1. Country-level analysis and the key participants of the network

Despite the high number of recent connectedness-related articles, there is limited insights about the different levels, changes in density and key participants (i.e., dominant factors). In this section, we use the net (outgoing–incoming) and sum connections to identify the core countries of the system, as shown in Table 4.

Aggregating the connections on a country level, the United States and Germany are at the top of the list. Our results align with the findings of Umar et al. (2022) and Berardi and Plazzi (2022) but we also consider cross-factor connections. They also claim that Japan and Great Britain are net importers of shock and hereby we confirm this statement.

Table 4 only provides an aggregated overview on a country level, however, to deeper understand our network, and identify the key participants, it is useful to aggregate on a node-level too, as they are driven by different economic effects. None of Sowmya et al. (2016) and Cavaca and Meurer (2021) or Gabauer et al. (2022) carry out this examination (as far as we know, we are the first to investigate this on the bond market), so hereby we extend their results. Nodes with the most connections are shown in Table 5. The first quarter of the table represents the summarized relations, whereas the subsequent columns show the nodes with the highest numbers of separate incoming and outgoing connections. For finding the dominating participants in our network we use net (outgoing–incoming) connections which is an accurate measurement according to Barigozzi and Brownlees (2019).

Table 5 highlights that in our network, the Slope factor of Canada has the most connections overall, at 32, from which 19 arrows originate and 13 come in. In a previous study, Umar et al. (2022) find that North-American countries have the most net connections in all subsystems. On 10-year Treasury bond yields, the results of Umar et al. (2020) show that the USA is the most dominant, followed by Canada, then the European countries. These findings are in line with our results, except we consider cross-connections too, in addition, in our case, all three factors of the USA lead the list of net connections.

Table 5
Key participants of the sovereign yield curve network.

Top 5 Sum				Top 5 Incoming		Top 5 Outgoing		Top 5 Net	
Node	Total	In	Out	Node	In	Node	Out	Node	Net
CAN S	32	13	19	ESP C	20	USA L	25	USA L	19
USA L	31	6	25	ITA C	19	USA C	22	USA C	15
AUS C	30	12	18	FRA C	18	USA S	20	USA S	11
AUS S	29	13	16	KOR L	14	CAN S	19	DEU L	9
DEU S	29	11	18	ITA S	14	DEU S	18	CAN L	8

To better comprehend the role of the USA sovereign yield curve in the network, we analyze the node-wise connections of the three factors. The connections of the USA Level, Slope, and Curvature components are highlighted in Fig. 3. The graphs support the statement of Table 5, while the US factors have few incoming connections, they have many outgoing ones. It is also visible that all three factors have numerous cross-connections (56.2% of the defined edges) which further emphasizes the importance of such relations.

The USA is not only dominant on a country level, as shown by Table 4, but on a node-wise level as well. Based on these outcomes, we conclude that relying on a static connectedness analysis, the US yield curve factors are the key participants of our the network. After the full-sample investigation, we examine the network behavior in turbulent (global and local crises) and tranquil periods.

5.2. Connectedness during different subperiods of the study horizon

The effects of crises on the sovereign yield curve networks are well documented in the empirical literature (Claeys and Vašíček, 2014; Reboredo and Ugolini, 2015), however, it is less common to compare different crises.[8] We examine the sovereign yield curve network in the crisis periods on different levels (yield curve factor, country, and node-wise) in a static way, then we investigate the networks in four previously discussed turbulent and tranquil periods to understand the differences between the global (GFC, C19) and local (DCB, ESDC) crises.

To deeper understand the different crises, we perform a static connectedness analysis on six separate time periods. Fig. 4 shows the periods introduced in Section 4, of which four are turbulent (2 globals and 2 locals) and two are calm.[9]

Fig. 4 highlights that C19 (763) and GFC (414) provide the networks with most connections, followed by DCB (236) and ESDC (234). The ratio of cross-connections is the following in each subperiod: DCB: 39.9%, CALM1: 57.8%, GFC: 62.6%, ESDC: 62.0%, CALM2: 62.7%, C19: 65.0%. These results further emphasize the importance of investigating cross-factor linkages.

The number of significant connections is higher in the two global crises (GFC, C19) than in local ones (DCB, ESDC), or calm periods. Fernández-Rodríguez et al. (2016), Chatziantoniou and Gabauer (2021) and Karkowska and Urjasz (2021) all find that in crisis periods the spillover is higher in the sovereign bond markets, which is in line with our results. We extend the contribution of the latter studies, by showing that while the density difference between calm periods and local crises is rather small, it is significantly larger during the two worldwide crises.

Similarly to the full-sample investigation, after identifying the density structures of the different time frames on yield curve factor level, we determine the countries that are responsible for the significant causal relations within the networks. The net connections for each subperiod, averaged by countries, are shown in Table A.7.

Except for the DCB period, the USA is the dominant country in each subperiod.[10] On a country level, the USA is the main exporter and Japan the main importer of interest rate shocks (apart from the cases of DCB and C19, when Japanese net connections add up to zero), which further emphasizes the findings of Berardi and Plazzi (2022).

To achieve a deeper understanding of the role of the key participants in the sovereign yield curve network during the selected periods, we aggregate the connections by nodes. Table 6 outlines the role of Level, Slope, and Curvature factors for the twelve countries. As far as we are aware, ours is the first paper that examines the roles of latent yield curve factors in calm, local and global crisis periods.

Considering the first column, we conclude that the majority of Level and Slope factors are net providers (7 out of 12 in both cases), while Curvatures are usually net recipients (8 out of 12) of causality relations. Based on Table 6 the USA is the only country

8 Previous articles such as Antonakakis and Vergos (2013), Fernández-Rodríguez et al. (2015, 2016), Hamill et al. (2021), Chatziantoniou and Gabauer (2021) and Umar et al. (2022) examine calm and turbulent periods, using a time frame that includes the Global Financial Crisis and the European Sovereign Debt Crisis while Karkowska and Urjasz (2021) and Umar et al. (2022) extend the investigation window to involve the Covid-19 pandemic as well. However, these papers only compare calm and turbulent periods with a dynamic model, and we widen their research twofold.

9 These periods range in length (DCB: 451 days, CALM1: 1770 days, GFC: 483 days, ESDC: 603 days, CALM2: 1787 days, C19: 510 days), so to maintain consistency, we first averaged the time span of the crises (512 days) and then pick such lengthy sets from the calm periods randomly (CALM1: 01/13/2004 - 12/28/2005; CALM2: 05/06/2014 - 04/20/2016). Our results are robust to the choice of the selected dates.

10 At the end of the '90s, South Korea (and other Southeastern Asian countries) went through a serious financial crisis and its consequences are felt during the 2000–2001 horizon which overlaps with the Dotcom Bubble in the US (Kihwan, 2006). Most of the net connections of South Korea in this period are due to the Level factor (15) which originates from the Bank of Korea's monetary policies described in Coe and Kim (2002) and Chung and Kim (2002).

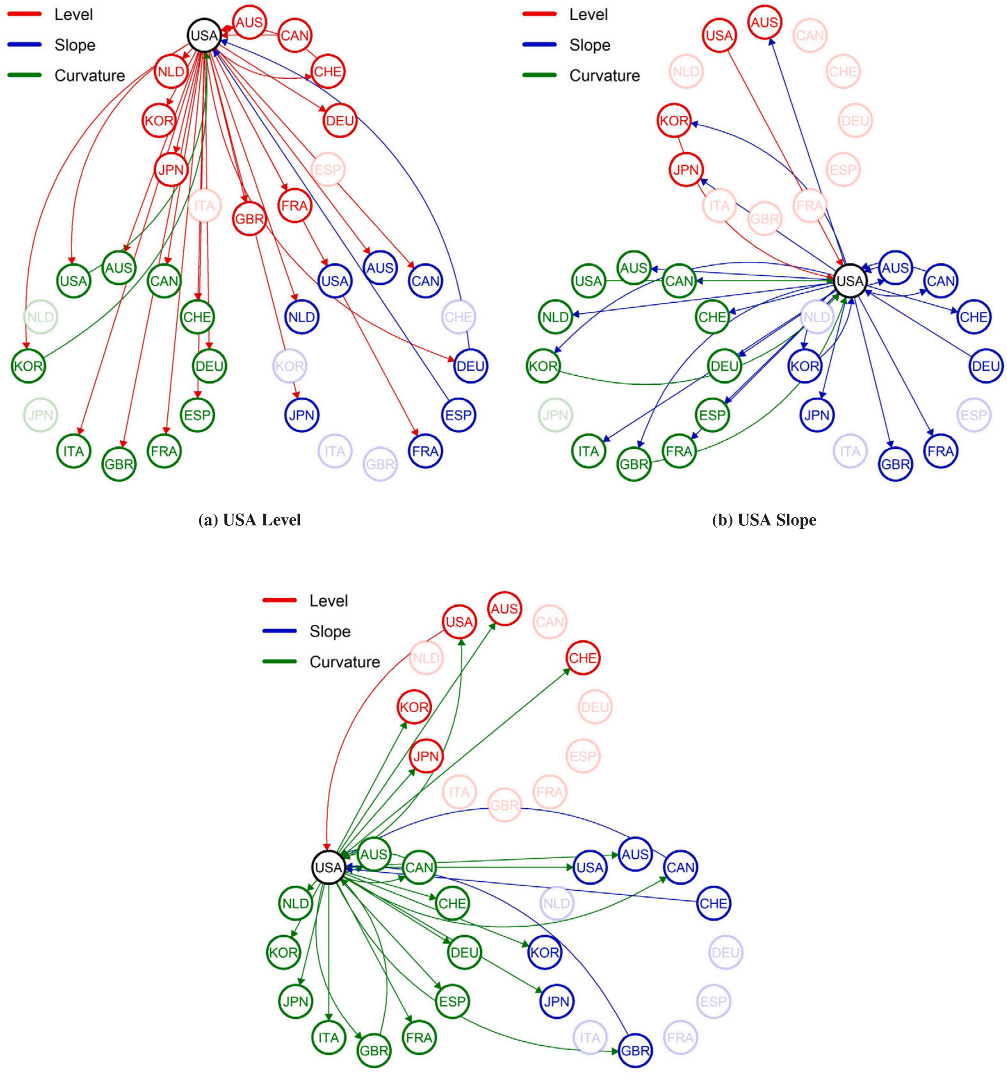

(a) USA Level **(b) USA Slope**

(c) USA Curvature

Fig. 3. Role of the USA nodes in the system, estimated by static Toda–Yamamoto model. Notes: Level factors are displayed in red, Slopes in blue, and Curvatures in green. An arrow between two factors indicates the direction of causation, and the color of the arrow indicates the source factor. Time series are differentiated at a maximum of one time, and the ideal lag time is chosen based on the AIC. For USA Level factors, 31 (44.29%); for Slope, 29 (41.43%); for Curvature 29 (41.43%) connections are significant from the total possible $70 = (2 \times (12 + 12 + 11))$. Cross-connection ratios are 67.7% for Level, 62.1% for Slope and 38.0% for Curvature. (For interpretation of the references to color in this figure legend, the reader is referred to the web version of this article.)

where all the three yield curve factors net connections are positive during each subperiod.[11] Table 6 confirms our previous statement, besides the US factors being the dominant nodes on the whole study period we claim that they are the key participants in every identified subperiods as well.

5.3. Dynamic, rolling-window-based connectedness analysis

Running a static analysis may not capture perfectly the cyclical and structural changes in the dynamics of the network and we are keen on exploring the potential changes in the network on different levels and the key participants through the examination horizon.

[11] In addition to the US factors, the Canadian Level and Slope have a high impact on the network for the majority of the time frame and Canada also can be found in a high position in the different subperiods in Table A.7. Greenwood-Nimmo et al. (2015) document that since Canada is a member of the North American Free Trade Agreement (NAFTA), it can be an indicator for being net positive in most cases.

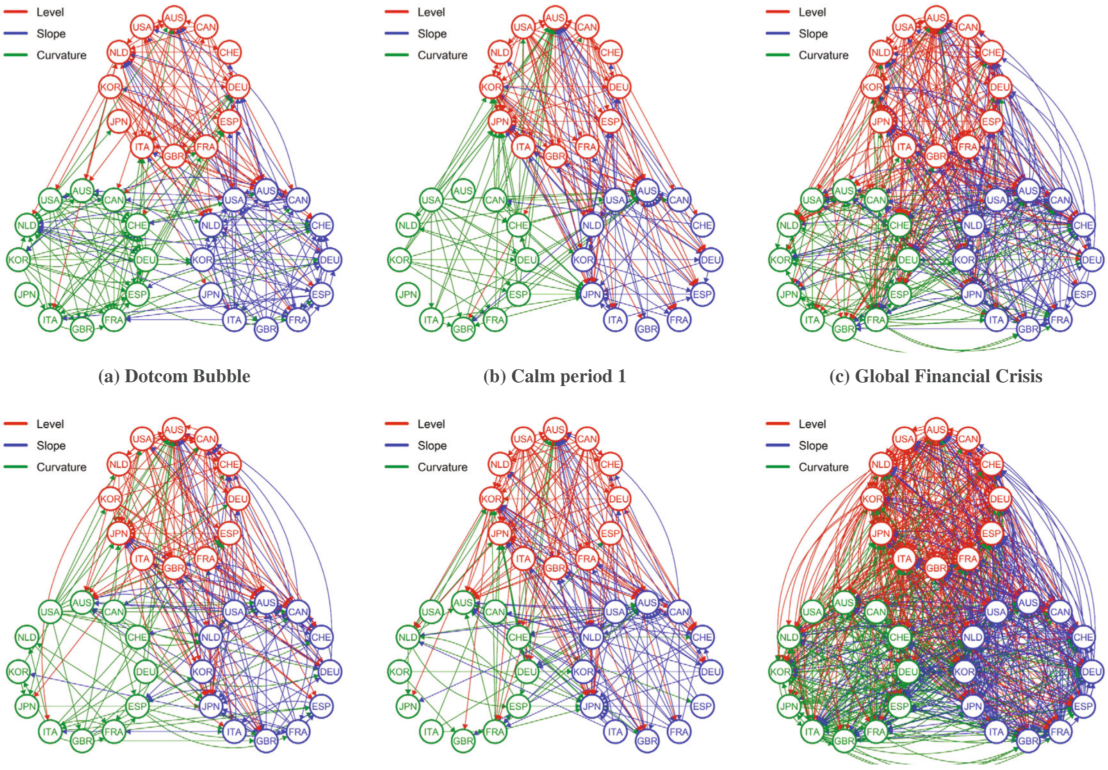

(a) Dotcom Bubble (b) Calm period 1 (c) Global Financial Crisis

(d) European Sovereign Debt Crisis (e) Calm Period 2 (f) Covid-19 Pandemic

Fig. 4. Network connectedness in different subperiods, estimated by static Toda–Yamamoto model. Notes: Level factors are displayed in red, Slopes in blue, and Curvatures in green. An arrow between two factors indicates the direction of causation, and the color of the arrow indicates the source factor. Time series are differentiated at a maximum of one time, and the ideal lag time is chosen based on the AIC. Number of connections in DCB: 236, in CALM1 (sample): 206, in GFC: 414, in ESDC: 234, in CALM2 (sample): 225, in C19: 763. (For interpretation of the references to color in this figure legend, the reader is referred to the web version of this article.)

Table 6
Factors being net transmitters or net receivers of causality connections during the six sub-periods.

	Level							Slope							Curvature						
	Whole period	DCB	CALM1	GFC	ESDC	CALM2	C19	Whole period	DCB	CALM1	GFC	ESDC	CALM2	C19	Whole period	DCB	CALM1	GFC	ESDC	CALM2	C19
AUS	+	−	−	−	−	−	−	+	−	−	+	−	−	−	+			−	−	−	−
CAN	+	+	+	+	+	+	+	+	+	+	+	−	+	+	−	+	+	+	+	+	+
CHE	+		+	−	−	+	+	+	−	+	−	−	−	−	+	−	+	−		+	−
DEU	+	−	−	+	+	+	+	+	−		−	−	+	−	+	+	+	+	+	+	−
ESP	+	−		+	+	+		−	+	−	+	−	+	+	−	−	+	−	+	+	−
FRA	+	+	+	+	+	+	+	−		−	−	+	+	−	−	+	+	+	−	+	−
GBR	−	+		+			+	+	+		+	−	−	−	−	−	−	−	+	−	
ITA		-	−	+	+	+	+	−	+		−	+	+	+	−	+	+	−	+	+	−
JPN	−	+	−	−	−	−	−	−	−	−	−	−	−	+	−			−	−	−	+
KOR	−	+	+	+	+	−	−	−	+	+	+	+	+	−	−	+	+	−		+	−
NLD	+	−	+	+	+	+	+	+	−	−	+	+	+	−	−	−	+	−	−	+	−
USA	+	+	+	+	+	+	+	+	+	+	+	+	+	+	+	+	+	+	+	+	+

Notes: + signs indicate that the factor is a net transmitter in the given period, while − signs indicate that the factor is a net receiver.

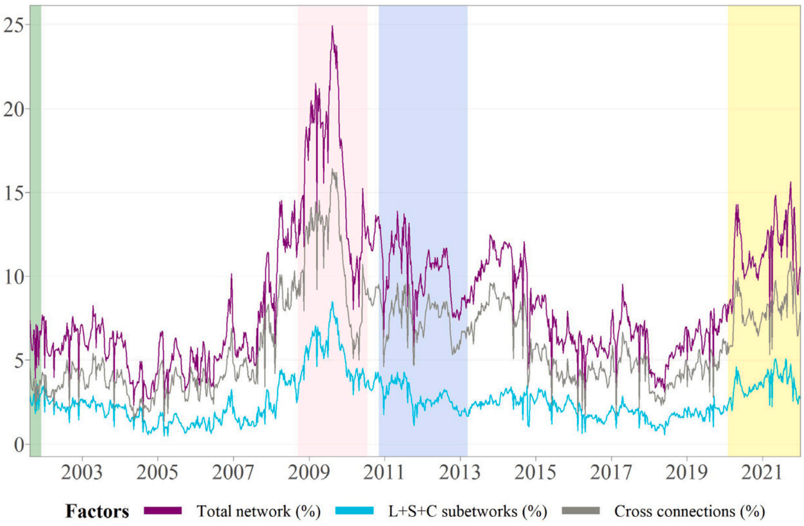

Fig. 5. Summarized connection ratios during the study period, estimated by dynamic Toda–Yamamoto model. Notes: Window size of 750 days and a lag determined by the AIC. The green area denotes the Dotcom Bubble, the red-shaded shows the Global Financial Crisis, the blue field represents the European Sovereign Debt Crisis, and the yellow covers the Covid-19 period. The purple line indicates the ratio of total significant connections, the cyan represents the summarized edges in the three subnetworks, and the gray line is the time series of the cross-connection ratios, compared to the maximum number of possible edges. (For interpretation of the references to color in this figure legend, the reader is referred to the web version of this article.)

Table 7
Average connection count by types during the six sub-periods — 750 days long window size.

	Whole period	DCB	CALM1	GFC	ESDC	CALM2	C19
L+S+C	32.4	34.2	24.3	67.4	35.1	25.9	44.9
Cross connections	75.5	43.4	54.3	139.7	93.1	65.9	100.3
All connections	108.0	77.6	78.6	207.1	128.2	91.8	145.3

Thus after the static examination, we perform a dynamic analysis of the sovereign yield curve network, similar to Sowmya et al. (2016), Cavaca and Meurer (2021), Umar et al. (2021a, 2022) and Gabauer et al. (2022).[12] We estimate 1064 different models as we roll the estimation window by one business week (5 days) through our sample. In Fig. 5 the purple, cyan, and gray lines represent the ratios of total significant connections, summarized edges in the three subnetworks, and the cross-connections, respectively compared to the maximum number of possible linkages.

The behavior of the three time series is very similar, and all of them peak during the GFC, and the C19 outbreak. In the empirical literature, there is general agreement that connectedness rises during turbulent times. The DCB and the ESDC cannot be viewed as a global phenomenon, thus the graphs in Fig. 5 do not indicate an upward tendency during these times. While Diebold and Yilmaz (2009), Billio et al. (2012) and Diebold and Yilmaz (2015) find this evidence for stocks, Antonakakis and Vergos (2013), Fernández-Rodríguez et al. (2015), Sowmya et al. (2016), Fernández-Rodríguez et al. (2016), Ahmad et al. (2018), Chatziantoniou and Gabauer (2021), Karkowska and Urjasz (2021), Hamill et al. (2021), Chatziantoniou and Gabauer (2021) and Umar et al. (2022) all exhibit the same on the bond markets. However, none of these studies differentiate between local and global crises (as far as we know, we are the first to investigate this on the bond market) so hereby we extend their results.

The average summarized connections for each subperiod are shown in Table 7.

Table 7 demonstrates that as the Level, Slope, and Curvature subnetworks get denser, cross-connections also increase during times of crisis.[13] Fig. 5 and Table 7 jointly show that the magnitude of cross-connections is around twice the combined number of connections in the yield curve factor subnetworks. Our dynamic analysis supports the results of the earlier studies of Sowmya et al. (2016), Cavaca and Meurer (2021), Umar et al. (2021a, 2022) and Gabauer et al. (2022), but we complete them with cross-connections between the Level, Slope and Curvature subnetworks.

[12] There is no exact rule to chose the sufficient window size and based on Arce et al. (2013) and Papana et al. (2017) we choose a rolling window method with 750 days. This can be seen as three years with 250 business days. In subsection B of the Appendix, we extend our analysis with window sizes of 500 and 1000 days. Furthermore, we perform a Granger causality test, with a rolling window size of 750 days, as an additional robustness check.

[13] A detailed view of the average edge counts by countries in these six periods is available in Table A.6 in the Appendix.

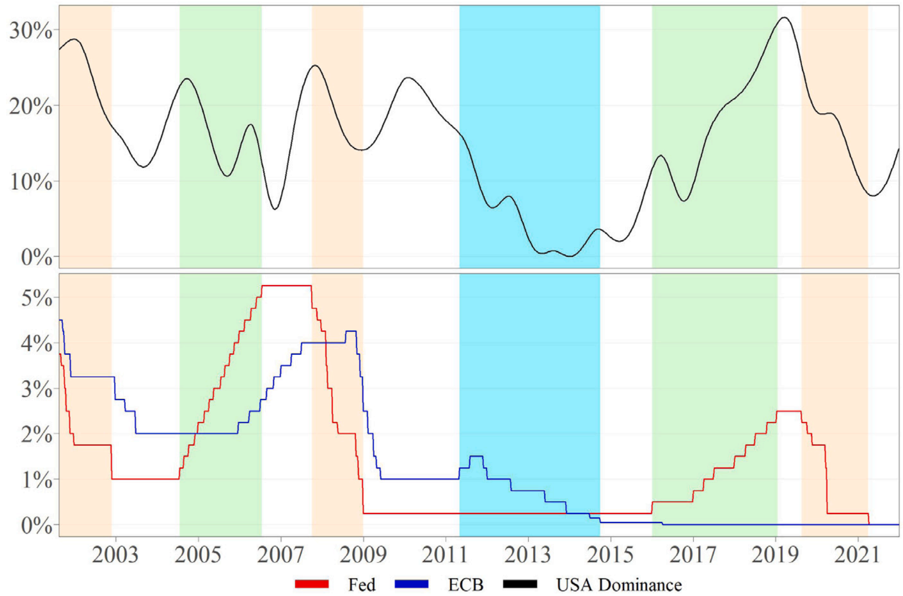

Fig. 6. Dynamic dominance of US factors, estimated by dynamic Toda–Yamamoto model. Notes: Window size of 750 days and a lag determined by the AIC, smoothed by cubic spline method. The orange areas denote the Fed interest rate cut, the green-shaded parts show Fed interest rate hikes and the cyan field represents the period when ECB leads the interest rate cycle. The red line stands for the Fed rates over time, while the blue represents ECB rates. The black line is the dynamic ratio of summarized outgoing USA edges and the total number of outgoing edges, smoothed by a cubic spline. (For interpretation of the references to color in this figure legend, the reader is referred to the web version of this article.)

5.4. The shift in the dominance of US factors across the study horizon

There is growing evidence in the empirical literature that US market shocks play a special role in international asset market comovements and Fed monetary policy affects the global bond market. Hofmann and Takáts (2015) are the first who document economically and statistically significant spillovers from the US short and long-term interest rates to advanced economies' government yields. In an influential paper (Miranda-Agrippino and Rey, 2020) study how the existence of a 'Global Financial Cycle' shapes the global financial spillovers of US monetary policy shocks. Lakdawala et al. (2021) also document that the Fed's communication on uncertainty regarding future actions is an additional, new monetary policy instrument through which the Fed can influence global financial conditions.

Empirical evidence on the effects of ECB policies on international government bonds is less clear (Jarociński, 2022). Kearns et al. (2018) find significant spillovers from ECB announcements and Curcuru et al. (2018) document that US and European government bond yields also co-move around these actions. Jarociński (2022) complete these results while he documents that spillovers of ECB interest rate shocks are smaller because they are conditional on the integration of European interest rates. Contrary to these findings, Miranda-Agrippino and Nenova (2022) document comparable magnitudes of spillovers related to the two central bank's monetary policy decisions. Based on these results, it is worth examining how the Fed and ECB monetary policy decisions affect the key participants of a sovereign bond-related network as well.

Hofmann and Takáts (2015), Albagli et al. (2019), Miranda-Agrippino and Rey (2020) and Lakdawala et al. (2021) all emphasize that the Fed exerts a significant impact on the rest of the world's fixed-income market through its monetary policy, which presents itself in a dominant role at the yield-curve factor level in our network. However, as evidenced by the lead–lag effect of the Fed's interest rate politics, based on Kearns et al. (2018), Jarociński (2022) and Miranda-Agrippino and Nenova (2022) this dominance can vary over time. Therefore we also examine the ECB monetary policy decisions.

In Sections 5.1 and 5.2 we show that the US factors are the key participants in our network, considering the whole time frame, as well as each subperiod. Upon further examination of the time series of these connections, based on Fig. B.3, we discover that these yield curve factors are the key participants of the system from a dynamic perspective too. Fig. B.3 highlights that the dominance of the US factors is time-varying; therefore, further economic drives can be behind these nodes' dynamics. Since monetary policy decisions have a great impact on the evolution of the yield curve, it is useful to investigate the linkage between the Fed's and ECB's easing and tightening decisions and the dominance of US factors.

In the lower part of Fig. 6 the time series of the policy rates set by the Federal Reserve (Fed, red line) and the European Central Bank (ECB, blue line) are visible.[14] Orange shading represents those periods when Fed cuts interest rates, while during green shading,

[14] The rates for the Fed and ECB are collected from https://fred.stlouisfed.org and https://www.ecb.europa.eu respectively.

Fed raises interest rates. Additionally, with cyan filling, the only period is noted when the ECB changes rates while the Fed does not. The upper part of Fig. 6 represents the ratio of the outgoing USA connections (Level, Slope, Curvature summarized) compared to the aggregated outgoing connections of the entire network. Fig. 6 shows that the Fed, in general, leads the ECB and this phenomenon is in line with the hypothesis that the Fed is the leader of the interest rate cycle. According to Brusa et al. (2020), the Fed is the global central bank and generally leads the other central banks in setting monetary policy.

Fig. 6 highlights that the US dominance decreases in the sovereign yield curve network when Fed cuts rates. Furthermore, its dominance reaches the global minimum when the interest rate cycle is led by the ECB (during the years 2011–2014). Based on Fig. 6, during interest rate hiking cycles, the dominance of the US factors also change, however, from 2016 to 2019, the dominance increased sharply, while a slight decrease is experienced between 2004 and 2006.

6. Concluding remarks

This study investigates the network of sovereign yield curves of 12 developed countries. We decompose the term structure of the interest rates into the Level, Slope, and Curvature factors using the dynamic Nelson and Siegel (1987) model as in Diebold and Li (2006). The connections between the latent yield curve across countries are measured using the Toda and Yamamoto (1995) method, which is suitable for cointegrated time series. Our examination also covers cross-factor relations. For deeper understanding the structural changes and identify the key participants in the sovereign yield curve network, we analyze the connections on factor, country, and node levels too. Our timeframe lasts over a 23-year long interval; therefore, we can compare two global (GFC and C19) and two local (DCB and ESDC) crises.

When considering the whole time period, the Slope subnetwork has the most connections of the three subsystems followed by Curvature and Level. Additionally, we claim that there is a significant amount of linkage between the three subnetworks on factor level, so cross-connections are not negligible. The number of total connections in the network increases during turbulent periods. During the two global crises (GFC and C19) the sovereign yield curve network is denser than in the two local (DCB, ESDC) cases. We found that the USA factors are the key participants in our network, considering the whole time frame, as well as each subperiod and the dynamic analysis too, but this behavior is time-varying. Although the dominance of the USA factors is independent of the characteristics of the subperiod (whether it is a calm, local or global crisis) it is affected by the Fed's and ECB's monetary policy decisions. The dominance of the US factors peaks if the Fed leads the hiking cycle and reaches its minimum when the interest rate cycle is led by the ECB.

Our results are relevant for academics, central bankers, and policy makers by providing insights into the behavior of sovereign yield curve networks during turbulent and tranquil periods. Our findings related to Fed and ECB monetary policy decisions are important for central bank policymaking. Identifying the key participants provides insights into the dynamics of the market. Specifically, monitoring the activities of these players can aid policymakers' assessment of the market conditions, identify potential risks, and detect any deviation from tranquil periods that may impact market stability. All network participants have linkages with various financial institutions and other asset classes, locally and globally. Policymakers need to be aware of these connections to assess systemic risk and the potential for contagion in times of market stress. Overall, our results about the influence of the Fed and the ECB, the two key players, can be useful for policymakers in smaller economies for managing their macroeconomic and monetary policy decisions. Essentially smaller economies have to be aware of their network exposure to key players to be prepared. Identifying the important players can help policymakers anticipate and mitigate the likely spillover effects emanating from disruptions or shocks from the key participants.

CRediT authorship contribution statement

Milan Csaba Badics: Conceptualization, Writing – original draft, Visualization. **Zsuzsa R. Huszar:** Supervision, Writing – review & editing. **Balazs B. Kotro:** Data curation, Methodology, Software, Visualization.

Data availability

The authors do not have permission to share data.

Appendix A. Supplementary data

Supplementary material related to this article can be found online at https://doi.org/10.1016/j.intfin.2023.101837.

References

Acemoglu, D., Ozdaglar, A., Tahbaz-Salehi, A., 2015. Systemic risk and stability in financial networks. Amer. Econ. Rev. 105 (2), 564–608.
Acharya, V., Engle, R., Richardson, M., 2012. Capital shortfall: A new approach to ranking and regulating systemic risks. Amer. Econ. Rev. 102 (3), 59–64.
Adrian, T., Brunnermeier, M.K., 2011. CoVaR. Technical Report, National Bureau of Economic Research.
Ahmad, W., Mishra, A.V., Daly, K.J., 2018. Financial connectedness of BRICS and global sovereign bond markets. Emerg. Mark. Rev 37, 1–16.
Albagli, E., Ceballos, L., Claro, S., Romero, D., 2019. Channels of US monetary policy spillovers to international bond markets. J. Financ. Econ. 134 (2), 447–473.
Almeida, C., Gomes, R., Leite, A., Simonsen, A., Vicente, J., 2009. Does curvature enhance forecasting? Int. J. Theor. Appl. Finance 12 (08), 1171–1196.
Alter, A., Beyer, A., 2014. The dynamics of spillover effects during the European sovereign debt turmoil. J. Bank. Financ. 42, 134–153.

Antonakakis, N., 2012. Exchange return co-movements and volatility spillovers before and after the introduction of euro. J. Int. Financ. Mark. Inst. Money 22 (5), 1091–1109.
Antonakakis, N., Vergos, K., 2013. Sovereign bond yield spillovers in the Euro zone during the financial and debt crisis. J. Int. Financ. Mark. Inst. Money 26, 258–272.
Arce, O., Mayordomo, S., Peña, J.I., 2013. Credit-risk valuation in the sovereign CDS and bonds markets: Evidence from the euro area crisis. J. Int. Money Finance 35, 124–145.
Barigozzi, M., Brownlees, C., 2019. Nets: Network estimation for time series. J. Appl. Econometrics 34 (3), 347–364.
Baruník, J., Křehlík, T., 2018. Measuring the frequency dynamics of financial connectedness and systemic risk. J. Financ. Econom. 16 (2), 271–296.
Batten, J.A., Choudhury, T., Kinateder, H., Wagner, N.F., 2022. Volatility impacts on the European banking sector: GFC and COVID-19. Ann. Oper. Res. 1–26.
Baumöhl, E., Bouri, E., Shahzad, S.J.H., Vỳrost, T., et al., 2022. Measuring systemic risk in the global banking sector: A cross-quantilogram network approach. Econ. Model. 109, 105775.
Benlagha, N., Hemrit, W., 2022. Does economic policy uncertainty matter to explain connectedness within the international sovereign bond yields? J. Econom. Finance 46 (1), 1–21.
BenSaïda, A., 2019. Good and bad volatility spillovers: An asymmetric connectedness. J. Financial Mark. 43, 78–95.
Berardi, A., Plazzi, A., 2022. Dissecting the yield curve: The international evidence. J. Bank. Financ. 134, 106286.
Bernal, O., Gnabo, J.-Y., Guilmin, G., 2014. Assessing the contribution of banks, insurance and other financial services to systemic risk. J. Bank. Finance 47, 270–287.
Bernal, O., Gnabo, J.-Y., Guilmin, G., 2016. Economic policy uncertainty and risk spillovers in the eurozone. J. Int. Money Finance 65, 24–45.
Bianchi, F., Mumtaz, H., Surico, P., 2009. The great moderation of the term structure of UK interest rates. J. Monetary Econ. 56 (6), 856–871.
Billio, M., Casarin, R., Costola, M., Pasqualini, A., 2016. An entropy-based early warning indicator for systemic risk. J. Int. Financ. Mark. Inst. Money 45, 42–59.
Billio, M., Getmansky, M., Lo, A.W., Pelizzon, L., 2012. Econometric measures of connectedness and systemic risk in the finance and insurance sectors. J. Financ. Econom. 104 (3), 535–559.
Bouri, E., Cepni, O., Gabauer, D., Gupta, R., 2021. Return connectedness across asset classes around the COVID-19 outbreak. Int. Rev. Financ. Anal. 73, 101646.
Bratis, T., Laopodis, N.T., Kouretas, G.P., 2020. Systemic risk and financial stability dynamics during the eurozone debt crisis. J. Financ. Stab. 47, 100723.
Bredin, D., O'Sullivan, C., Spencer, S., 2021. Forecasting WTI crude oil futures returns: Does the term structure help? Energy Econ. 100, 105350.
Brusa, F., Savor, P., Wilson, M., 2020. One central bank to rule them all. Rev. Finance 24 (2), 263–304.
Bubák, V., Kočenda, E., Žikeš, F., 2011. Volatility transmission in emerging European foreign exchange markets. J. Bank. Financ. 35 (11), 2829–2841.
Byrne, J.P., Cao, S., Korobilis, D., 2019. Decomposing global yield curve co-movement. J. Bank. Financ. 106, 500–513.
Cavaca, I.B., Meurer, R., 2021. International monetary policy spillovers: Linkages between US and South American yield curves. Int. Rev. Econ. Finance 76, 737–754.
Cavaliere, G., Rahbek, A., Taylor, A.R., 2010. Cointegration rank testing under conditional heteroskedasticity. Econom. Theory 26 (6), 1719–1760.
Chatziantoniou, I., Gabauer, D., 2021. EMU risk-synchronisation and financial fragility through the prism of dynamic connectedness. Q. Rev. Econ. Finance 79, 1–14.
Christensen, J.H., Rudebusch, G.D., 2012. The response of interest rates to US and UK quantitative easing. Econ. J. 122 (564), F385–F414.
Christiansen, C., 2007. Volatility-spillover effects in European bond markets. Eur. Financial Manag. 13 (5), 923–948.
Chung, C.-S., Kim, S.-J., 2002. New evidence on high interest rate policy during the Korean crisis. Korean Crisis Recovery 137.
Claeys, P., Vašíček, B., 2014. Measuring bilateral spillover and testing contagion on sovereign bond markets in Europe. J. Bank. Financ. 46, 151–165.
Clarke, J.A., Mirza, S., 2006. A comparison of some common methods for detecting Granger noncausality. J. Stat. Comput. Simul. 76 (3), 207–231.
Coe, M.D.T., Kim, M.S.-J., 2002. Korean Crisis and Recovery. International Monetary Fund.
Corsi, F., Lillo, F., Pirino, D., Trapin, L., 2018. Measuring the propagation of financial distress with granger-causality tail risk networks. J. Financ. Stab. 38, 18–36.
Curcuru, S.E., De Pooter, M., Eckerd, G., 2018. Measuring Monetary Policy Spillovers Between US and German Bond Yields. FRB International Finance Discussion Paper 1226.
De Pooter, M., 2007. Examining the Nelson-Siegel class of term structure models: In-sample fit versus out-of-sample forecasting performance. Available at SSRN 992748.
De Santis, R.A., Zimic, S., 2018. Spillovers among sovereign debt markets: Identification through absolute magnitude restrictions. J. Appl. Econometrics 33 (5), 727–747.
Demirer, M., Diebold, F.X., Liu, L., Yilmaz, K., 2018. Estimating global bank network connectedness. J. Appl. Econometrics 33 (1), 1–15.
Dewachter, H., Lyrio, M., 2006. Macro factors and the term structure of interest rates. J. Money Credit Bank. 119–140.
Diebold, F.X., Li, C., 2006. Forecasting the term structure of government bond yields. J. Econometrics 130 (2), 337–364.
Diebold, F.X., Rudebusch, G.D., Aruoba, S.B., 2006. The macroeconomy and the yield curve: a dynamic latent factor approach. J. Econometrics 131 (1–2), 309–338.
Diebold, F.X., Yilmaz, K., 2009. Measuring financial asset return and volatility spillovers, with application to global equity markets. Econ. J. 119 (534), 158–171.
Diebold, F.X., Yilmaz, K., 2012. Better to give than to receive: Predictive directional measurement of volatility spillovers. Int. J. Forecast. 28 (1), 57–66.
Diebold, F.X., Yılmaz, K., 2014. On the network topology of variance decompositions: Measuring the connectedness of financial firms. J. Econometrics 182 (1), 119–134.
Diebold, F.X., Yilmaz, K., 2015. Trans-Atlantic equity volatility connectedness: US and European financial institutions, 2004–2014. J. Financ. Econom. 14 (1), 81–127.
Dolado, J.J., Lütkepohl, H., 1996. Making Wald tests work for cointegrated VAR systems. Econometr. Rev. 15 (4), 369–386.
Elliott, M., Golub, B., Jackson, M.O., 2014. Financial networks and contagion. Amer. Econ. Rev. 104 (10), 3115–3153.
Engle, R.F., Granger, C.W., 1987. Co-integration and error correction: representation, estimation, and testing. Econometrica 251–276.
Engsted, T., Tanggaard, C., 1994. Cointegration and the US term structure. J. Bank. Financ. 18 (1), 167–181.
Evans, C.L., Marshall, D.A., 2007. Economic determinants of the nominal treasury yield curve. J. Monetary Econ. 54 (7), 1986–2003.
Fernández-Rodríguez, F., Gómez-Puig, M., Sosvilla-Rivero, S., 2015. Volatility spillovers in EMU sovereign bond markets. Int. Rev. Econ. Finance 39, 337–352.
Fernández-Rodríguez, F., Gómez-Puig, M., Sosvilla-Rivero, S., 2016. Using connectedness analysis to assess financial stress transmission in EMU sovereign bond market volatility. J. Int. Financ. Mark. Inst. Money 43, 126–145.
Gabauer, D., Subramaniam, S., Gupta, R., 2022. On the transmission mechanism of Asia-Pacific yield curve characteristics. Int. J. Finance Econ. 27 (1), 473–488.
Gai, P., Haldane, A., Kapadia, S., 2011. Complexity, concentration and contagion. J. Monetary Econ. 58 (5), 453–470.
Gai, P., Kapadia, S., 2010. Contagion in financial networks. Proc. R. Soc. Lond. Ser. A Math. Phys. Eng. Sci. 466 (2120), 2401–2423.
Glasserman, P., Young, H.P., 2015. How likely is contagion in financial networks? J. Bank. Financ. 50, 383–399.
Gómez-Puig, M., Sosvilla-Rivero, S., 2013. Granger-causality in peripheral EMU public debt markets: A dynamic approach. J. Bank. Financ. 37 (11), 4627–4649.
Gómez-Puig, M., Sosvilla-Rivero, S., 2016. Causes and hazards of the euro area sovereign debt crisis: Pure and fundamentals-based contagion. Econ. Model. 56, 133–147.
Granger, C.W., 1969. Investigating causal relations by econometric models and cross-spectral methods. Econometrica 424–438.
Greenwood-Nimmo, M., Nguyen, V.H., Shin, Y., 2015. Measuring the connectedness of the global economy.

Gunay, S., 2021. Comparing COVID-19 with the GFC: A shockwave analysis of currency markets. Res. Int. Bus. Finance 56, 101377.
Gündüz, Y., Kaya, O., 2014. Impacts of the financial crisis on eurozone sovereign CDS spreads. J. Int. Money Finance 49, 425–442.
Hall, A.D., Anderson, H.M., Granger, C.W., 1992. A cointegration analysis of treasury bill yields. Rev. Econom. Statist. 116–126.
Hamill, P.A., Li, Y., Pantelous, A.A., Vigne, S.A., Waterworth, J., 2021. Was a deterioration in 'connectedness'a leading indicator of the European sovereign debt crisis? J. Int. Financ. Mark. Inst. Money 74, 101300.
Hautsch, N., Schaumburg, J., Schienle, M., 2015. Financial network systemic risk contributions. Rev. Finance 19 (2), 685–738.
Hofmann, B., Takáts, E., 2015. International monetary spillovers. BIS Q. Rev. Sept..
Hué, S., Lucotte, Y., Tokpavi, S., 2019. Measuring network systemic risk contributions: A leave-one-out approach. J. Econom. Dynam. Control 100, 86–114.
Jana, R.K., Ghosh, I., Goyal, V., 2022. Spillover nexus of financial stress during black swan events. Finance Res. Lett. 48, 102892.
Jarociński, M., 2022. Central bank information effects and transatlantic spillovers. J. Int. Econ. 139, 103683.
Jebabli, I., Kouaissah, N., Arouri, M., 2022. Volatility spillovers between stock and energy markets during crises: A comparative assessment between the 2008 global financial crisis and the COVID-19 pandemic crisis. Finance Res. Lett. 46, 102363.
Ji, Q., Bouri, E., Roubaud, D., Shahzad, S.J.H., 2018. Risk spillover between energy and agricultural commodity markets: A dependence-switching CoVaR-copula model. Energy Econ. 75, 14–27.
Ji, Q., Liu, B.-Y., Fan, Y., 2019. Risk dependence of CoVaR and structural change between oil prices and exchange rates: A time-varying copula model. Energy Econ. 77, 80–92.
Johansen, S., 1988. Statistical analysis of cointegration vectors. J. Econom. Dynam. Control 12 (2–3), 231–254.
Kang, S.H., McIver, R., Yoon, S.-M., 2017. Dynamic spillover effects among crude oil, precious metal, and agricultural commodity futures markets. Energy Econ. 62, 19–32.
Karkowska, R., Urjasz, S., 2021. Connectedness structures of sovereign bond markets in Central and Eastern Europe. Int. Rev. Financ. Anal. 74, 101644.
Kearns, J., Schrimpf, A., Xia, F.D., 2018. Explaining monetary spillovers: The matrix reloaded. J. Money Credit Bank..
Kihwan, K., 2006. The 1997-98 Korean financial crisis: Causes, policy response, and lessons. In: IMF Seminar on Crisis Prevention in Emerging Markets.
Koopman, S.J., Mallee, M.I., Van der Wel, M., 2010. Analyzing the term structure of interest rates using the dynamic Nelson–Siegel model with time-varying parameters. J. Bus. Econom. Statist. 28 (3), 329–343.
Lakdawala, A., Moreland, T., Schaffer, M., 2021. The international spillover effects of US monetary policy uncertainty. J. Int. Econ. 133, 103525.
Mensi, W., Boubaker, F.Z., Al-Yahyaee, K.H., Kang, S.H., 2018. Dynamic volatility spillovers and connectedness between global, regional, and GIPSI stock markets. Finance Res. Lett. 25, 230–238.
Miranda-Agrippino, S., Nenova, T., 2022. A tale of two global monetary policies. J. Int. Econ. 136, 103606.
Miranda-Agrippino, S., Rey, H., 2020. The global financial cycle after lehman. In: AEA Papers and Proceedings, Vol. 110. pp. 523–528.
Miranda-Agrippino, S., Ricco, G., 2021. The transmission of monetary policy shocks. Am. Econ. J.: Macroecon. 13 (3), 74–107.
Mönch, E., 2012. Term structure surprises: the predictive content of curvature, level, and slope. J. Appl. Econometrics 27 (4), 574–602.
Mumtaz, H., Surico, P., 2009. Time-varying yield curve dynamics and monetary policy. J. Appl. Econometrics 24 (6), 895–913.
Nazlioglu, S., Gupta, R., Bouri, E., 2020. Movements in international bond markets: The role of oil prices. Int. Rev. Econ. Finance 68, 47–58.
Nelson, C.R., Siegel, A.F., 1987. Parsimonious modeling of yield curves. J. Business 473–489.
Nucera, F., Schwaab, B., Koopman, S.J., Lucas, A., 2016. The information in systemic risk rankings. J. Empir. Financ. 38, 461–475.
Papana, A., Kyrtsou, C., Kugiumtzis, D., Diks, C., 2017. Financial networks based on granger causality: A case study. Physica A 482, 65–73.
Pittis, N., 1999. Efficient estimation of cointegrating vectors and testing for causality in vector autoregressions. J. Econ. Surv. 13 (1), 1–35.
Rambaldi, A.N., Doran, H.E., 1996. Testing for Granger Non-Casuality in Cointegrated Systems Made Easy. Department of Econometrics, University of New England.
Reboredo, J.C., Ugolini, A., 2015. Systemic risk in European sovereign debt markets: A CoVaR-copula approach. J. Int. Money Finance 51, 214–244.
Rossi, B., 2005. Optimal tests for nested model selection with underlying parameter instability. Econometr. Theory 21 (5), 962–990.
Rossi, B., Wang, Y., 2019. Vector autoregressive-based granger causality test in the presence of instabilities. Stata J. 19 (4), 883–899.
Sander, H., Kleimeier, S., 2003. Contagion and causality: an empirical investigation of four Asian crisis episodes. J. Int. Financ. Mark. Inst. Money 13 (2), 171–186.
Sedunov, J., 2016. What is the systemic risk exposure of financial institutions? J. Financ. Stab. 24, 71–87.
Sowmya, S., Prasanna, K., Bhaduri, S., 2016. Linkages in the term structure of interest rates across sovereign bond markets. Emerg. Mark. Rev 27, 118–139.
Stenfors, A., Chatziantoniou, I., Gabauer, D., 2022. Independent policy, dependent outcomes: A game of cross-country dominoes across European yield curves. J. Int. Financ. Mark. Inst. Money 81, 101658.
Stona, F., Caldeira, J.F., 2019. Do US factors impact the Brazilian yield curve? Evidence from a dynamic factor model. North Amer. J. Econom. Finance 48, 76–89.
Toda, H.Y., Yamamoto, T., 1995. Statistical inference in vector autoregressions with possibly integrated processes. J. Econometrics 66 (1–2), 225–250.
Ullah, W., Matsuda, Y., Tsukuda, Y., 2015. Generalized Nelson–Siegel term structure model: do the second slope and curvature factors improve the in-sample fit and out-of-sample forecasts? J. Appl. Stat. 42 (4), 876–904.
Umar, Z., Kenourgios, D., Papathanasiou, S., 2020. The static and dynamic connectedness of environmental, social, and governance investments: International evidence. Econ. Model. 93, 112–124.
Umar, Z., Riaz, Y., Aharon, D.Y., 2022. Network connectedness dynamics of the yield curve of G7 countries. Int. Rev. Econ. Finance 79, 275–288.
Umar, Z., Riaz, Y., Zaremba, A., 2021a. Spillover and risk transmission in the components of the term structure of eurozone yield curve. Appl. Econ. 53 (18), 2141–2157.
Umar, Z., Trabelsi, N., Zaremba, A., 2021b. Oil shocks and equity markets: The case of GCC and BRICS economies. Energy Econ. 96, 105155.
Van Dijk, D., Koopman, S.J., Van der Wel, M., Wright, J.H., 2014. Forecasting interest rates with shifting endpoints. J. Appl. Econometrics 29 (5), 693–712.
Vỳrost, T., Lyócsa, Š., Baumöhl, E., 2015. Granger causality stock market networks: Temporal proximity and preferential attachment. Physica A 427, 262–276.
Wilms, I., Croux, C., 2016. Forecasting using sparse cointegration. Int. J. Forecast. 32 (4), 1256–1267.
Xu, X., Chen, C.Y.-H., Härdle, W.K., 2019. Dynamic credit default swap curves in a network topology. Quant. Finance 19 (10), 1705–1726.
Yu, W.-C., Zivot, E., 2011. Forecasting the term structures of Treasury and corporate yields using dynamic Nelson-Siegel models. Int. J. Forecast. 27 (2), 579–591.
Zapata, H.O., Rambaldi, A.N., 1997. Monte Carlo evidence on cointegration and causation. Oxford Bull. Econom. Statist. 59 (2), 285–298.